

# We are IntechOpen, the world's leading publisher of Open Access books Built by scientists, for scientists

6,900

Open access books available

186,000

International authors and editors

200M

Downloads

Our authors are among the

154

Countries delivered to

TOP 1%

most cited scientists

12.2%

Contributors from top 500 universities



WEB OF SCIENCE™

Selection of our books indexed in the Book Citation Index  
in Web of Science™ Core Collection (BKCI)

Interested in publishing with us?  
Contact [book.department@intechopen.com](mailto:book.department@intechopen.com)

Numbers displayed above are based on latest data collected.  
For more information visit [www.intechopen.com](http://www.intechopen.com)



## Blood Perfusion Models for Infrared Face Recognition

Shiqian Wu, Zhi-Jun Fang, Zhi-Hua Xie and Wei Liang  
*School of information technology, Jiangxi University of Finance and Economics,  
 China*

### 1. Introduction

Infrared (IR) technology has traditionally been applied to military use and remote sensing. During the last two decades, the cost of IR cameras (especially uncooled imagers) has been significantly reduced with the development of CCD technology, and therefore civil applications have increased constantly due to its unique features. One of such applications is IR face recognition (Prokoski et al., 1992, Prokoski, 2000, Kong et al., 2005). The fundamentals behind it are, as indicated by Kong et al (Kong et al., 2005) that IR images are independent of external illumination. While visible images represent the reflectance information of the face surface, IR face images contain more fundamental information about faces themselves, such as anatomical information (Prokoski, et al., 1992, Prokoski, 2000); the thermal characteristics of faces with variations in facial expression and make-up remain nearly invariant (Socolinsky & Selinger, 2002) and the tasks of face detection, localization, and segmentation are relatively easier and more reliable than those in visible images (Kong et al., 2005). It has been pointed by Prokoski et al. (Prokoski et al., 1992) that humans are homoiotherm and hence capable of maintaining constant temperature under different surroundings. The thermal images collected over 20 years have demonstrated that the thermal measurements of individuals are highly repeatable under the same conditions. Furthermore, as discussed by Prokoski (Prokoski, 2000), a facial thermal pattern is determined by the vascular structure of each face, which is irreproducible and unique.

Based on the assumption that facial thermal patterns are determined by blood vessels transporting warm blood, Prokoski tried to extract the blood vessel minutiae (Prokoski, 2001) or vascular network (Buddharaju et al., 2004, Buddharaju et al., 2005) as the facial features for recognition. The basic idea is to extract such features using image segmentation. It has been indicated by Guyton & Hall (Guyton & Hall, 1996) that the average diameter of blood vessels is around 10~15 $\mu$ m, which is too small to be detected by current IR cameras (limited by the spatial resolution); the skin directly above a blood vessel is on average 0.1°C warmer than the adjacent skin, which is beyond the thermal accuracy of current IR cameras. The methods using image segmentation in (Prokoski, 2001, Buddharaju et al., 2004, Buddharaju et al., 2005) are heuristic, and it still remains a big challenge to capture the pattern of blood vessels on each face.

On the other hand, the phenomenon of “homoiotherm” due to human temperature regulation has led to the direct use of thermograms for recognition (Wilder et al., 1996,

Source: Recent Advances in Face Recognition, Book edited by: Kresimir Delac, Mislav Grgic and Marian Stewart Bartlett, ISBN 978-953-7619-34-3, pp. 236, December 2008, I-Tech, Vienna, Austria

Socolinsky & Selinger, 2002, Wu et al., 2003, Chen et al., 2005). Wilder et al. (Wilder et al., 1996) used three different feature-extraction and decision-making algorithms for test. The recognition results revealed that both visible and IR imageries perform similarly across algorithms. The real-time IR face recognition system developed by Wu et al. (Wu et al., 2003) achieves good performance. Especially, Socolinsky & Selinger (Socolinsky & Selinger, 2002) simultaneously registered the IR and visible images of each candidate under controlled conditions. It has been concluded from their experimental results that (1) variations of IR images are less than those of visible images; (2) IR images are less sensitive to facial expression changes. The experiments conducted with the common methods like principle component analysis (PCA), linear discriminant analysis (LDA), local feature analysis (LFA) and independent component analysis (ICA) demonstrated that using thermal infrared imagery yields higher performance than using visible images under many circumstances (Socolinsky & Selinger, 2002).

It is noted that the aforementioned database mainly involved same-session data (i.e., nearly-simultaneous acquisition of training and testing data). Besides the same-session test, Chen et al. (Chen et al., 2005) paid more attention to test of time-lapse data (i.e., training data and testing data being collected in different time sessions). The intervals among training data and testing data are several weeks, several months or even one year respectively. The large-scale studies involving both same-session and time-lapse data indicated that in a same-session scenario, neither modality is significantly better than the other using the PCA-based recognition; however, using visible imagery outperforms that using IR imagery for time-lapse data.

When we mention that humans are homoiothermal, it should be highlighted that the so called “homoiotherm” only refers to the approximately constant temperature in deep body (i.e., the core temperature), whereas the skin temperature distribution fluctuates with the ambient temperature, changes from person to person, and from time to time, as shown in (Houdas & Ring, 1982, Guyton & Hall, 1996, Jones & Plassmann, 2000). It should also be noted that an IR camera can only capture the apparent temperature instead of deep temperature. As indicated by Houdas & Ring (Houdas & Ring, 1982), the variations in facial thermograms result from not only external conditions, such as environmental temperature, imaging conditions, but also various internal conditions, such as physiological or psychological conditions. Socolinsky & Selinger (Socolinsky & Selinger, 2004A, Socolinsky & Selinger, 2004B) also explored such variations.

To improve the performance of IR face recognition for time-lapse session, more efforts have been put on classifier design (Socolinsky & Selinger, 2004A, Socolinsky & Selinger, 2004B, Srivastava & Liu, 2003). Meanwhile, some researchers focus on feature extraction. Yoshitomi et al. (Yoshitomi et al., 1997) used both thermal information and geometrical features for recognition. Wu et al. (Wu et al., 2005A) proposed a model to convert the thermograms to blood perfusion data and the performance on time-lapse data is significantly improved. The modified blood perfusion model by Wu et al. (Wu et al., 2007) further improves the time-lapse performance.

In this chapter, we will provide a comprehensive study on the proposed blood perfusion models. It is revealed that the transforms by the blood perfusion models reduce the within-class scatter of thermograms and obtains more consistent features to represent human faces. In the following Section, the thermal pattern variations are analyzed. The blood perfusion models are presented and analyzed in Section 3. A variety of experiments on blood perfusion and thermal data are performed in Section 4, and the conclusions are drawn in Section 5.

## 2. Thermal pattern variations and analysis

Although IR images are independent of illumination, fluctuations in thermal appearance occur in relation to ambient conditions, subject's metabolism and so on. It is necessary to learn how the thermal patterns vary in different situations before presenting the proposed methods. Some of the factors affecting thermal distribution are presented in the following subsections.

### 2.1 Deep body temperature vs skin temperature

In 1958, Aschoff and Wever introduced the terms "thermal core", the temperatures of which remain almost exactly constant, within  $\pm 0.6^{\circ}\text{C}$ , day in and day out except when a person develops a febrile illness (Guyton & Hall, 1996). Blatteis (Blatteis, 1998) indicates that even if ambient temperature varies widely, core temperature does not change as a function of ambient temperature. This is due to the presence of a closed control loop with negative feedback in the body system which prevents mean body temperature from deviating extensively from this value taken under thermoneutral conditions (Blatteis, 1998). In fact, a rise in core temperature of only  $0.5^{\circ}\text{C}$  causes extreme peripheral vasodilation (flushing of the skin in humans). This stability implies that the heat produced in the body and that lost from it stay in relative balance, despite the large variations in ambient temperature (Blatteis, 1998).

The skin temperature, in contrast to the core temperature, fluctuates with the temperature of the surroundings (Guyton & Hall, 1996, Blatteis, 1998). One may infer, therefore, that in order to maintain core temperature stable, the rate of heat flow from core to skin is adjusted according to the body's thermal needs and that, as a result, skin temperature varies more widely than core temperature in relation to ambient temperature (Blatteis, 1998). Under steady-state conditions in a thermoneutral environment, (i.e., one in which neither the mechanism for heat production nor for heat loss is activated and the perceived thermal comfort is optimal), core temperature thus is higher than skin temperature (Blatteis, 1998). For resting, naked adults, this zone of ambient temperature lies between  $28$  and  $30^{\circ}\text{C}$  (Blatteis, 1998).

There is no single temperature level that can be considered to be normal because measurements on many normal people have shown a *range* of normal temperature measured orally, from less than  $36.1^{\circ}\text{C}$  to  $37.5^{\circ}\text{C}$  (Guyton & Hall, 1996). When excessive heat is produced in the body by strenuous exercise, temperature can rise temporarily to as high as  $38.33$ - $40.0^{\circ}\text{C}$ . On the other hand, when the body is exposed to cold, the temperature can often fall to values below  $96^{\circ}\text{F}$  ( $35.56^{\circ}\text{C}$ ) (Guyton & Hall, 1996).

### 2.2 Variation with ambient conditions

The works by Chen et al. (Chen et al., 2005), Socolinsky & Selinger (Socolinsky & Selinger, 2004A, Socolinsky & Selinger, 2004B), Wu et al. (Wu et al., 2005A, Wu et al., 2007) have illustrated that variations in ambient temperature significantly change the thermal characteristics of faces, and accordingly affect the performances of recognition. Fig. 1 shows the thermal distribution of the same face in different ambient temperatures. All of the images are observed (the red part) from the pixel values ranging from 238 to 255. It is observed from Fig.1 that the skin temperature of the cheeks, tip of nose and hair increases as the ambient temperature increases. The intensities of the forehead region start off as bright when the ambient temperature is low. As the ambient temperature increases (above  $27.9^{\circ}\text{C}$  ~  $28.1^{\circ}\text{C}$ ), the intensities of the forehead region drops drastically due to the effect of sweating. It was indicated by Blatteis (Blatteis, 1998) that the human body has about three million sweat glands, the greatest density being found on the palms, soles and forehead. Thermoregulatory sweating

increases with elevation in core temperature (Blatteis, 1998), and therefore the forehead region emits sweat easily when the ambient temperature increases. Evaporation takes place once the sweat reaches the surface, hence causing the skin temperature to lower down.

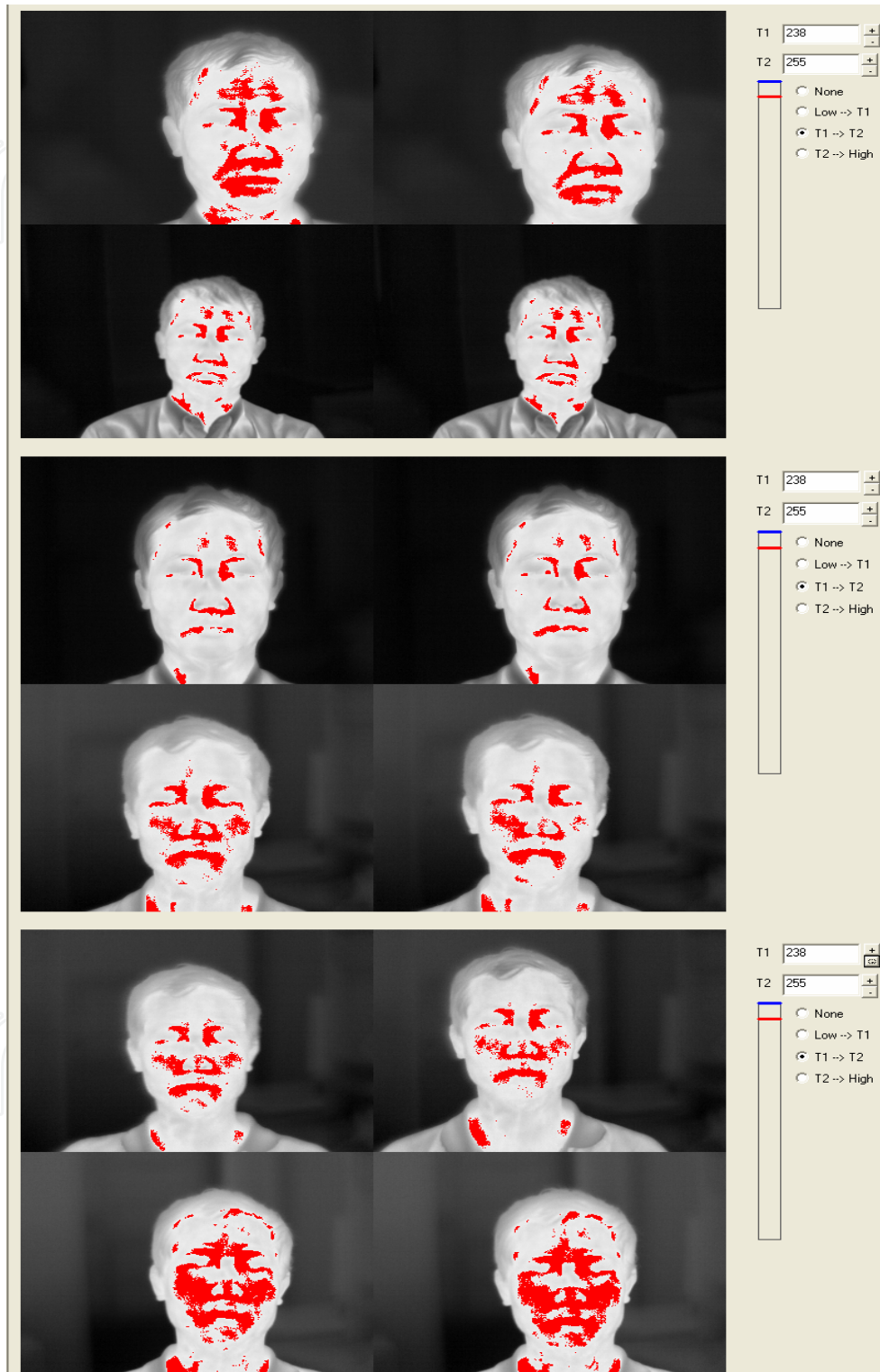
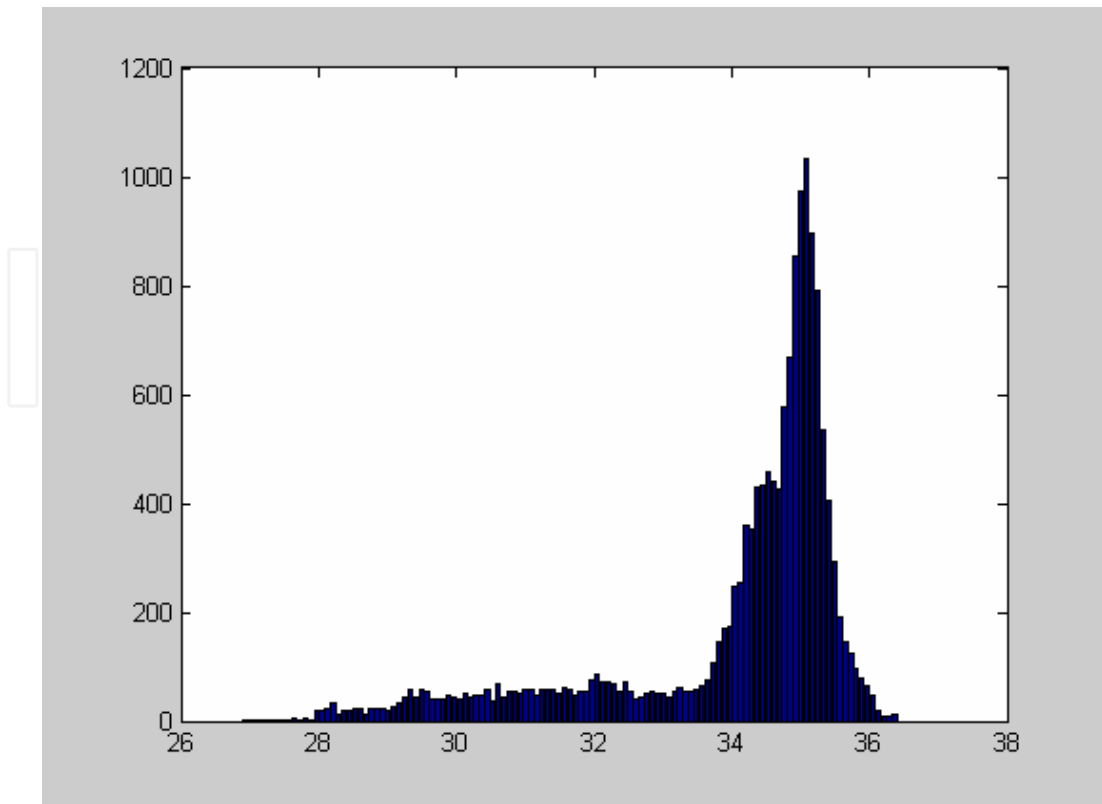
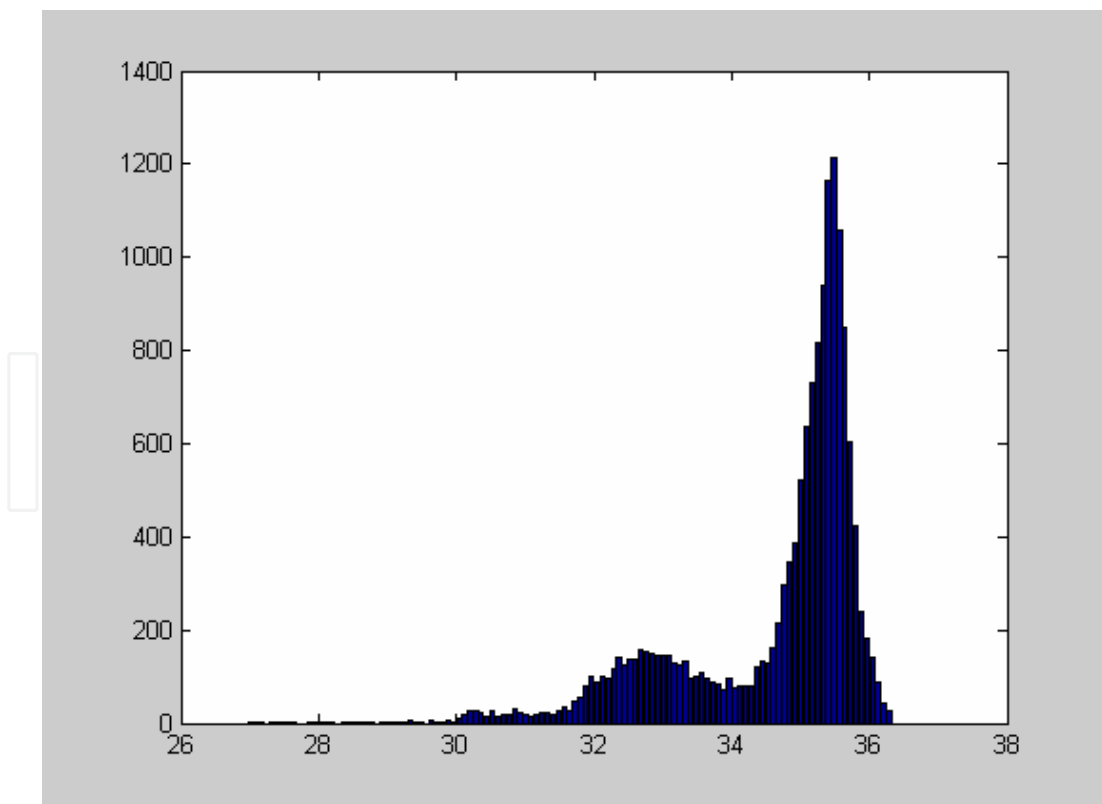


Fig. 1. Images taken at different ambient conditions (1st row: 24.8 °C ~ 25.0 °C, 2nd row: 25.7 °C ~ 26.1 °C, 3th row: 27.1 °C ~ 27.4 °C, 4th row: 27.9 °C ~ 28.1 °C, 5th row: 28.4 °C ~ 28.7 °C, 6th row: 28.9 °C ~ 29.3 °C)



(a) Histogram in ambient temperature 24.8 °C ~ 25.0 °C



(b) Histogram in ambient temperature 28.9 °C ~ 29.3 °C

Fig. 2. Histograms in different ambient temperatures of the same face

### 2.3 Variation due to metabolism

Ganong (Ganong, 2001) indicates that the body temperature is lowest during sleep, slightly higher in the awake but relaxed state, and rises with activity. For activities such as exercising, the heat produced by muscular contraction accumulates in the body and cause the body temperature to rise (Ganong, 2001).

Body temperature also rises slightly during emotional excitement, probably owing to unconscious tensing of the muscles (Ganong, 2001). It is chronically elevated by as much as 0.5 °C when the metabolic rate is high, as in hyperthyroidism, and lowered when the metabolic rate is low, as in hypothyroidism (Ganong, 2001). There is an additional monthly cycle of temperature variation characterized by a rise in basal temperature at the time of ovulation for women (Ganong, 2001). Temperature regulation is less precise in young children, and they may normally have a temperature that is 0.5 °C or so above the established norm for adults (Ganong, 2001).

Socolinsky & Selinger (Socolinsky & Selinger, 2004A, Socolinsky & Selinger, 2004B) also analysed that additional fluctuations in thermal appearance could be related to the subject's metabolism. During their data collection, an uncontrolled portion of the subjects was engaged in strong physical activity at different periods prior to imaging. The time elapsed from physical exertion to imaging was uncontrolled and known to be different for different sessions. This further contributes to the change in thermal appearance.

### 2.4 Variation due to breathing patterns

Fig.3 shows the images when the person is breathing in (the first one), breathing out (the middle one) and no breathing (last one), and the curve below represents the reversed cumulative histograms. The curves in red, green and blue represent the subject breathing in,

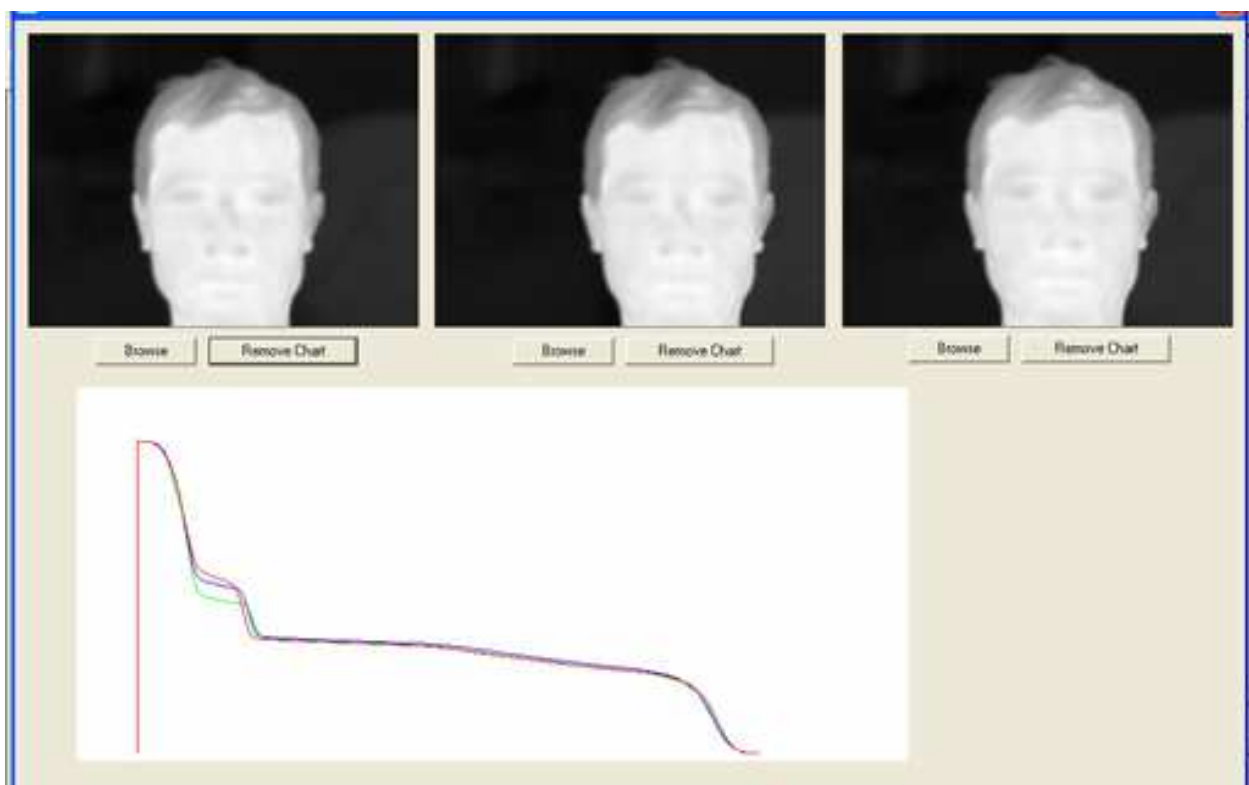


Fig. 3. Reversed cumulative histogram for inhalation & exhalation

breathing out and no breathing respectively. It can be seen that a relatively larger area of the face is subjected to low temperature (left part in the curve) when the subject breathes in and high temperature when breathes out. The area of the face with higher temperature part (right part in the curve) stays almost constant regardless of whether the subject is breathing in or out. Such change is obvious: when the subject exhales, the region directly below nose (i.e., region around nose and mouth) becomes warmer since exhaled air is at core body temperature, which is several degrees warmer than skin temperature.

## 2.5 Variation due to alcohol consumption

The variation in thermal distribution when the subject is under alcohol consumption is shown in Fig.4. It is generally known that alcohol increases body temperature because it dilates blood vessels in the skin. The flushed complexion associated with drinking is due to central vasomotor depression. In Fig.4, the top left image is taken immediately after consumption of alcohol, the top right image is taken 15 min later after consumption, bottom left image is taken after 35 min delay and finally the bottom right image is taken 100 min later. It can be observed that there are changes in the appearance of the thermal images at different timings after a single session of drinking alcohol. More regions of the face, especially the cheeks and forehead became warm as time passes after consumption. This is due to the fact that alcohol concentration in the blood flowing in the human face peaked only some time after consumption.

Alcohol consumption can normally affect thermal distribution for each individual differently. It depends on the amount of dosage and how fast the rate of absorption of alcohol takes place in the body. The rate of absorption can in turn be determined by whether there was any food consumption beforehand or whether the subject had his / her pyloric valves removed surgically (Goodwin, 2000).



Fig. 4. Images taken at different timings after alcohol consumption

Actually, many other factors affect the thermograms. These include imaging condition (e.g., thermal drift, distance, glasses etc), psychological condition (e.g., angry, blushing, stress etc) and physiological condition (toothache, headache etc). As indicated by Jones & Plassmann (Jones & Plassmann, 2000), “the skin temperature distribution changes from person to person, and from time to time”. It is difficult to extract the unique features of a face.

### 3. Blood perfusion models

It is assumed that the ambient condition is stable without wind and sun effect, and the subjects are in the steady state without temperature regulation, i.e., the following assumptions are made:

Assumption 1: The deep body temperature is constant, and no thermal regulation (e.g., sweating) is considered;

Assumption 2: The ambient temperature is lower than body temperature (e.g., indoor condition is considered);

Assumption 3: Pathological conditions (e.g., fever, headache, inflammation, etc) and psychological conditions (e.g., anger, blush, etc) are not considered.



(a) Thermal data ( $T_e = 26.2^\circ\text{C}$ );



(b) Corresponding blood perfusion data

Fig. 5. Thermal data vs blood perfusion data

In view of the heat transfer and thermal physiology under these assumptions, the heat transfer on skin surface can be described by the following heat equilibrium equations (Houdas & Ring, 1982):

$$H_r + H_e + H_f = H_c + H_m + H_b \quad (1)$$

where  $H$  represents the heat flux per unit area. The subscripts  $r$ ,  $e$  and  $f$  stand for radiation, evaporation and convection respectively. These three terms on left hand are the outflows which point from the skin surface to the environment. The subscripts  $c$ ,  $m$  and  $b$  stand for body conduction, metabolism and blood flow convection. These are the influx terms in the direction from the body to the skin surface. Based on the analysis in (Wu et al., 2005A), blood perfusion is expressed as follows:

$$\omega = \frac{\varepsilon\sigma(T_s^4 - T_e^4) + A\mu d^{3M-1}(P g\beta/\nu^2)^M (T_s - T_e)^{M+1} - k(T_c - T_s)/D - H_m}{\alpha c_b(T_a - T_s)} \quad (2)$$

where the specific parameters are tabulated in Table 1. Equation (2) defines the thermogram to blood perfusion transform, with which a thermal datum  $T(x, y)$  at location  $(x, y)$  can be therefore converted into the corresponding blood perfusion  $\omega(x, y)$ . An example of the conversion is shown in Fig. 5.

symbol	description	Value
$\omega$	Blood perfusion	
$\sigma$	Stefan-Boltzmann constant	$5.67*10^{-8} \text{ W m}^{-2}\text{K}^{-4}$
$\varepsilon$	Tissue/ skin thermal emissivity	0.98
$T_s$	Skin temperature	
$T_e$	Ambient temperature	
$T_a$	Artery temperature	312.15K
$T_c$	Core temperature	312.15K
$k$	tissue/ skin thermal conductivity	$0.2\text{Wm}^{-1}\text{K}^{-1}$
$\mu$	Air thermal conductivity	$0.024 \text{ W m}^{-1}\text{K}^{-1}$
$c_b$	blood specific heat	$3.78*10^3 \text{ Jkg}^{-1} \text{ K}^{-1}$
$H_m$	metabolic heat flux per unit area	$4.186\text{W m}^{-2}$
$\alpha$	tissue/ skin countercurrent exchange ratio	0.8
$P$	Prandtl constant	0.72
$\nu$	kinematic viscosity of air	$1.56*10^{-5} \text{ m}^2/\text{s}$
$\beta$	air thermal expansion coefficient	$3.354*10^{-3}\text{K}^{-1}$
$g$	local gravitational acceleration	$9.8\text{m}^2/\text{s}$
$A$	constant	0.27
$M$	constant	0.25
$d$	Characteristic length of a face	0.095
$D$	Distance from body core to skin surface	0.095

Table 1. Nomenclature

The proposed blood perfusion model by equation (2) defines a transform from the thermal space to the blood perfusion space. It is a point-wise transform and has the following characteristics: the location of the facial features is preserved; the shape of the subject is identical to the thermograms. It is noted that the concept of blood perfusion is meaningful only for skin part; for the non-skin part (e.g., hair and background), it could be viewed as an equivalent "blood perfusion".

It is easy to derive the differential of blood perfusion to temperature  $T$  as follows:

$$\frac{d\omega}{dT} = \frac{[4\varepsilon\sigma T^3 + A\mu d^{3M-1}(P g\beta/\nu^2)^M (T - T_e)^M + kT/D](T_c - T) + S}{\alpha c_b(T_a - T)^2} \quad (3)$$

where

$$S = \varepsilon\sigma(T^4 - T_e^4) + A\mu d^{3M-1}(Pg\beta/v^2)^M(T - T_e)^{M+1} - k(T_c - T)/D - H_m \quad (4)$$

As  $T > T_e$  according to Assumption 2,  $T_a > T$ , and  $S$  is always positive since the blood perfusion is positive,  $\frac{d\omega}{dT}$  is definitely positive. This implies that the relationship between the skin temperature  $T$  and the blood perfusion  $\omega$  is monotonous. The skin area with relatively high temperature results in high blood perfusion as demonstrated in Fig.5. From the perspective of image processing, the proposed transform is a nonlinear one, as can be seen from Fig. 6. In essence, it increases the dynamic range of IR images and enhances the overall image contrast as visually demonstrated in Fig. 5. More specific and also importantly, it expands the contrast on high-temperature part (i.e., skin) and suppresses the contrast on low-temperature part (i.e., hair, background, etc.). As mentioned in Section 2, the thermal variations are usually big in low-temperature part due to environmental changes, but very small in high-temperature part because of the temperature regulation. Since the high-temperature part is the most meaningful portion of the signal for the decision making, the proposed blood-perfusion-based transform is appropriate since it overcomes the inherent variations in thermogram data.

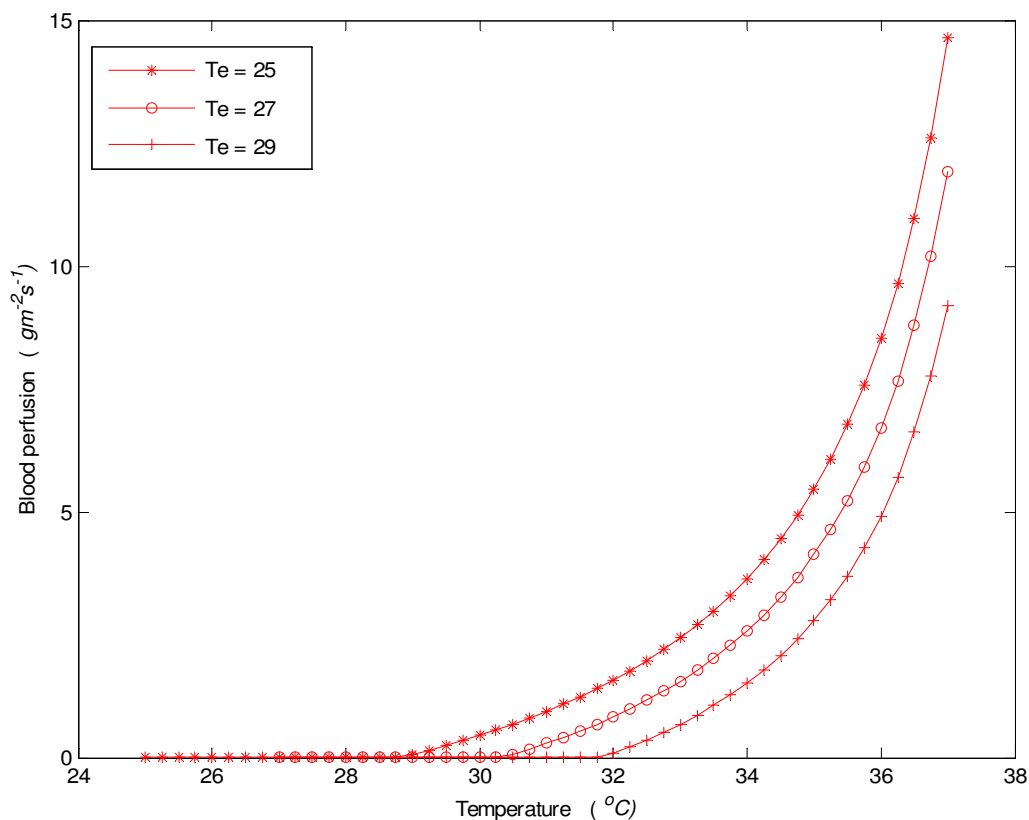


Fig. 6. The relationship between temperature data and blood perfusion data

Using the parameters shown in Table 1, it is found that  $H_f$  has much less effect (second-order effect) on blood perfusion than  $H_r$ . If  $T_e$  has a change  $\Delta T_e$ , and we neglect the small variation of  $H_f$ , we have:

$$\Delta\omega \approx \frac{\varepsilon\sigma T^4}{\alpha c_b(T_a - T)} \left\{ \left[ 1 - \left( \frac{T_e}{T} \right)^4 \right] - \left[ 1 - \left( \frac{T_e + \Delta T_e}{T} \right)^4 \right] \right\} \tag{5}$$

i.e.,

$$\Delta\omega \approx \zeta \left[ \left( \frac{T_e + \Delta T_e}{T} \right)^4 - \left( \frac{T_e}{T} \right)^4 \right] \tag{6}$$

where

$$\zeta = \varepsilon\sigma T^4 / \alpha c_b(T_a - T) \tag{7}$$

Expanding equation (6):

$$\Delta\omega \approx \zeta \left[ 4 \frac{T_e^3}{T^3} \frac{\Delta T_e}{T} + 6 \frac{T_e^2}{T^2} \left( \frac{\Delta T_e}{T} \right)^2 + 4 \frac{T_e}{T} \left( \frac{\Delta T_e}{T} \right)^3 + \left( \frac{\Delta T_e}{T} \right)^4 \right] \tag{8}$$

If  $\Delta T_e / T$  is small (note: the unit of  $T$  is Kelvin temperature), and ignore the high-order terms, we obtain:

$$\Delta\omega \approx 4\zeta \frac{T_e^3}{T^4} \Delta T_e \tag{9}$$

It reveals from equation (9) that if  $T_e$  has a small variation, the change of blood perfusion is almost linear, which is illustrated in Fig. 7. However, the gradient for each point is the function of its temperature.

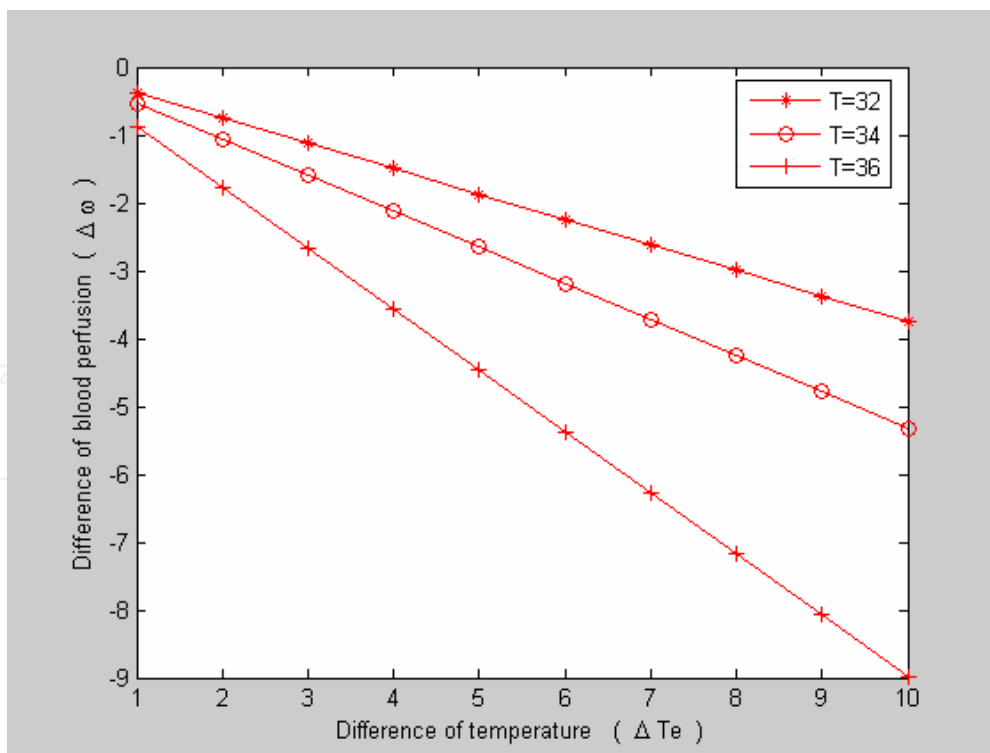


Fig. 7. The difference of blood perfusions vs different ambient temperatures ( $T_e = 23^{\circ}C$ ) Let  $\eta = 4\zeta T_e^3 / T^4$ , which determines the transform from the  $\Delta T_e$  to  $\Delta\omega$ , and use equation (7), we have:

$$\eta = 4 \frac{\varepsilon \sigma T_e^3}{\alpha c_b (T_a - T)} \quad (10)$$

Using the parameters specified in Table 1, and setting  $T_e = 15 \sim 30^\circ C$ , and  $T = 32 \sim 36^\circ C$ , the variations of parameter  $\eta$  are demonstrated in Fig. 8. It is observed that the smaller  $T$  and  $T_e$  are, the smaller  $\eta$  is. Even when  $T_e = 30^\circ C$  and  $T = 36^\circ C$ ,  $\eta$  is less than 0.7. This implies that if the ambient temperature has variation  $\Delta T_e$ , the resultant variation of blood perfusion  $\Delta \omega$  is always less than  $\Delta T_e$ . Hence, from the perspective of pattern recognition, the transform in equation (2) reduces the within-class scatter resulting from ambience, and obtains more consistent data to represent the human face.

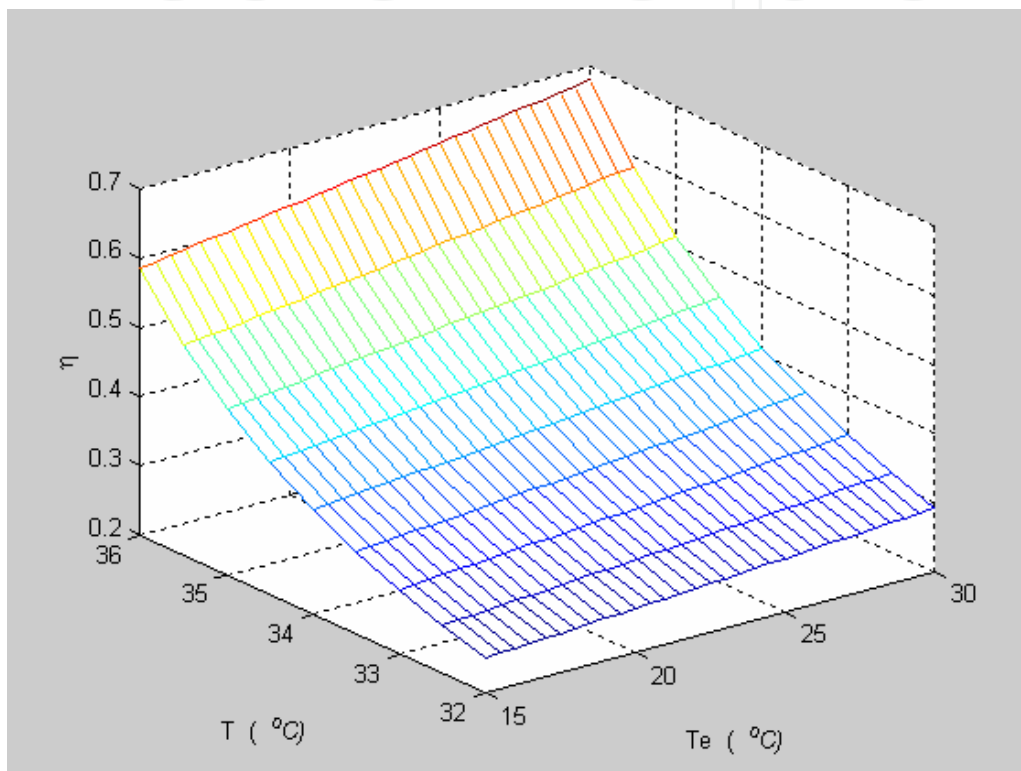


Fig. 8. The transform coefficient  $\eta$  from  $\Delta T_e$  to  $\Delta \omega$  in different temperatures

It should be highlighted that some parameters, for example  $M$ ,  $D$ ,  $d$  etc., described in equation (2) are obtained from experiments. These values should vary or differ from person to person instead of constants as shown in Table 1. Furthermore, it is found that terms  $H_f$ ,  $H_c$ ,  $H_m$  and  $H_e$  are less significant compared to other terms. Therefore, it is reasonable to ignore these terms to obtain a simplified blood perfusion model as follows:

$$\omega = \frac{\varepsilon \sigma (T^4 - T_e^4)}{\alpha c_b (T_a - T)} \quad (11)$$

For convenience, we call equation (2) as complex blood perfusion model or original blood perfusion (OBP) model and equation (11) as modified blood perfusion (MBP) model. The relationship between the two models is depicted in Fig. 9. It is observed that both models have similar properties, for example, nonlinear and monotonous increase, but with different gradients.

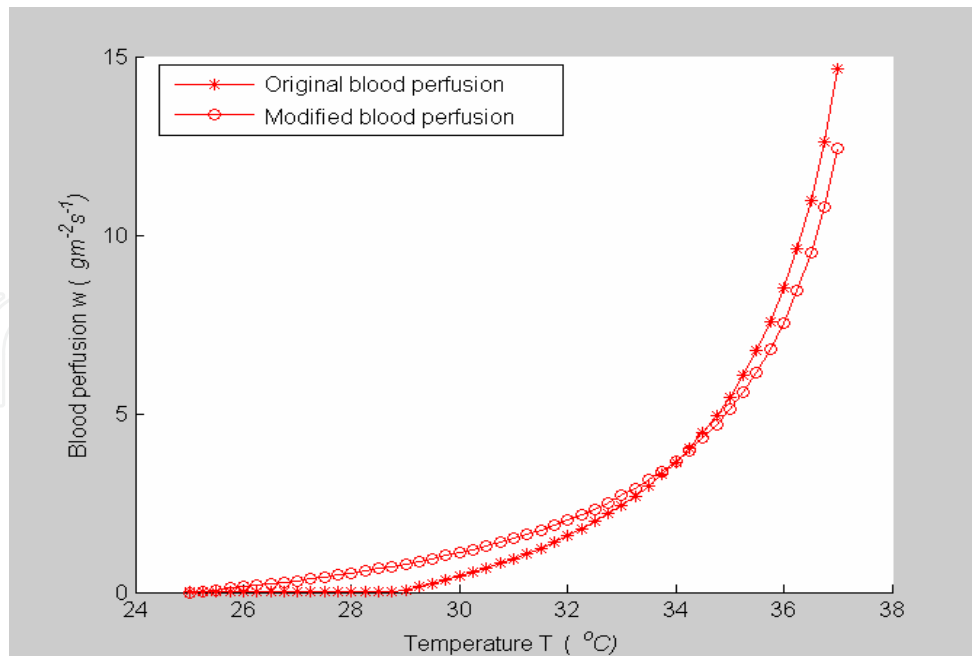


Fig. 9. Original blood perfusion model vs modified blood perfusion model

## 4. Experimental results

### 4.1 IR face recognition system

The experiments were performed using the real-time IR face recognition system as described in (Wu et al., 2003). The schematic diagram of the system is shown in Fig.10. After an image is captured, its quality is evaluated by an objective measurement (Wu et al., 2005B). Only the image with good quality is inputted to the following detection and then recognition modules. Before normalize the face in a specific size, the face orientation is detected by single linkage clustering (Wu et al. 2006). Then, the facial features are extracted by the principle component analysis and Fisher's linear discriminant method, and the classifier employs the RBF neural network as shown in (Wu et al. 2003) for details. The performance is evaluated in terms of maximum recognition score.

### 4.2 Database collection

The IR images were captured by the ThermoVision A40 made by FLIR Systems Inc. This camera, which uses an uncooled microbolometer sensor with resolution of 320×240 pixels and the spectral response is 7.5 ~ 13 microns, is specially designed for accurate temperature measurement. The sensitivity is as high as 0.08 °C. One of its prominent features is the function of automatic self-calibration to cope with the temperature drift. Furthermore, we have a blackbody MIKRON M340 to check and compensate the accuracy of measurement. The database used in experiments comprises 850 data of 85 individuals which were carefully collected at the same condition: i.e., same environment under air-conditioned control with temperature around 24.3 ~ 25.3°C, and each person stood at a distance of about 1 meter in front of the camera. Each person has 10 templates: 2 in frontal-view, 2 in up-view, 2 in down-view, 2 in left-view, and 2 in right-view. All the 10 images of each subject were acquired within 1 minute. As glass is opaque to IR, people are required to remove their eyeglasses.

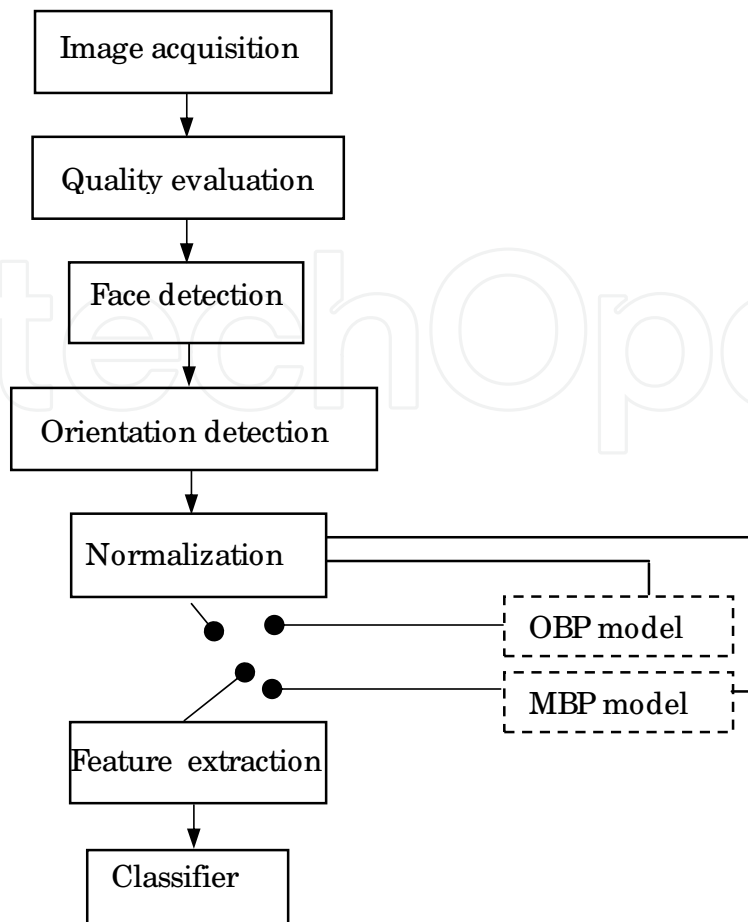


Fig. 10. Schematic diagram of the IR face recognition system

#### 4.3 Recognition results for same-session data

The test situation is similar to the watchlist scenario described in FRVT 2002 (Bone & Blackburn, 2002). The subject is allowed to walk slowly back and forth in front of the camera at a distance between 0.7m and 1.4m. He/ she may have different poses and facial expressions. For different purposes, the subjects were asked to wear/ remove eyeglasses.

##### A. Effect of eyeglasses

During the first part of this experiment, the subjects were required to remove their eyeglasses. These testing images were captured right after collecting the training data. Here, the numbers of subjects and probe images are 10 and 114 respectively.

Immediately after the first part of the experiment, the same group of testing persons was instructed to put on their eyeglasses for the next round of image capturing. The number of probe images is 108. The recognition results performed on thermal data, original blood perfusion (OBP) model and modified blood perfusion (MBP) model are tabulated in Table 2 and Table 3. The recognition scores are demonstrated in Fig.11 and Fig. 12 respectively.

Ambient Condition	Thermal	OBP	MBP
24.3 °C – 25.3 °C	data	model	model
Recognition Rate	96.4%	100%	100%
Mean Score	0.825	0.913	0.874
Variance	0.299	0.289	0.280

Table 2. Recognition rate for same-session data without eyeglasses

Ambient Condition	Thermal	OBP	MBP
24.3 °C – 25.3 °C	data	model	Model
Recognition Rate	80.9%	91.7%	91.7%
Mean Score	0.705	0.803	0.764
Variance	0.448	0.418	0.437

Table 3. Recognition rate for same-session data with eyeglasses

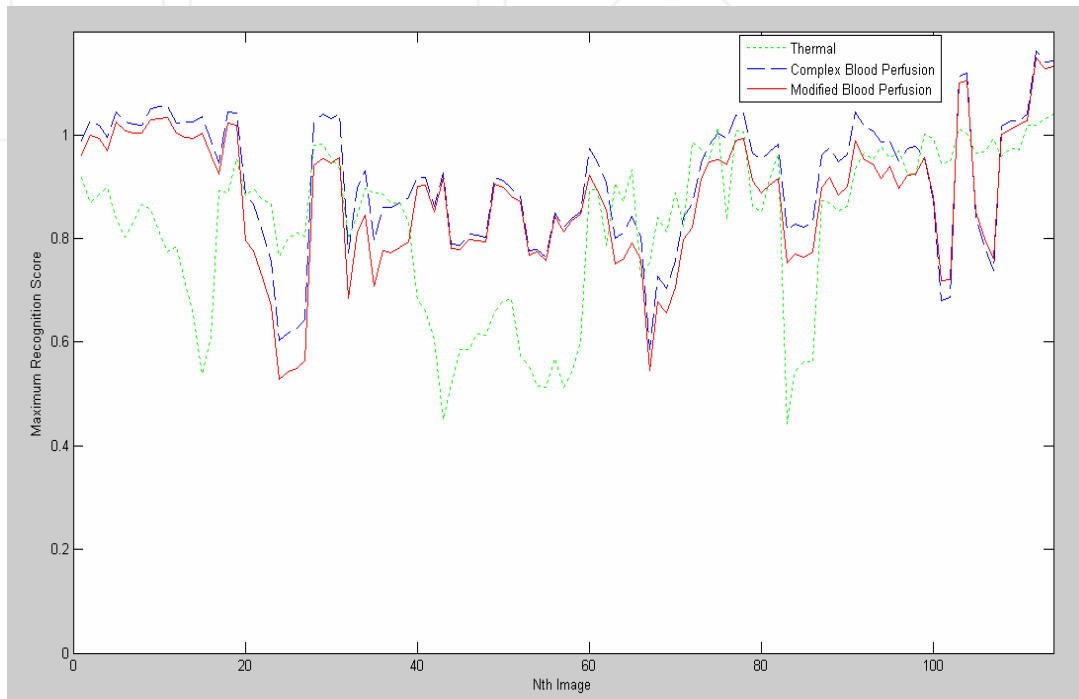


Fig. 11. Maximum recognition score for same-session data without eyeglasses

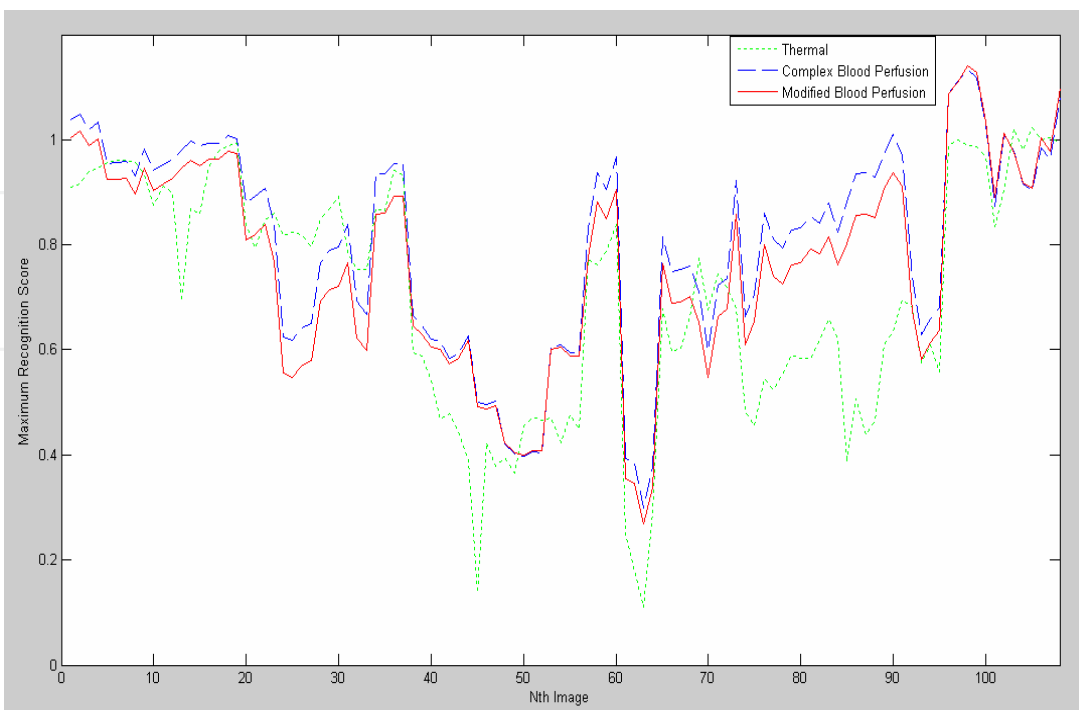


Fig. 12. Maximum recognition score for same-session data with eyeglasses

From Table 2, it can be seen that the recognition rates for both blood perfusion models are excellent (achieved 100% recognition rate). The maximum recognition scores obtained are generally high for all the three models. The small variances indicate that the performances are robust. It is observed from Table 3 that wearing eyeglasses leads to decrease of recognition rate, especially for thermal images. The effects on OBP model and MBP model are similar and both the blood perfusion models greatly outperform the thermal model in terms of recognition rates and scores.

### B. Effect of ambient temperature & metabolism

In this experiment, 15 subjects were engaged in some physical activity prior to imaging. They came to register their images in the afternoon between 1 p.m. to 4 p.m. The outdoor condition on that day was a warm and sunny weather, with ambient temperature ranging around 28.3 °C– 29.5 °C, while the indoor temperature is around 25.1 °C– 25.3 °C. There are totally 150 probe images collected. In this case, body temperature has significantly changes due to different activities and ambient temperatures. Accordingly, the performance in this situation decreases in terms of the recognition rates, recognition scores and score variances as shown in Table 4 and Fig.13, although the interval between training and testing is around 2 minutes. As discussed in Section 2, the thermal characteristics indeed change under

Ambient Condition 28.3°C – 29.5 °C to 25.1 °C– 25.3 °C	Thermal data	OBP model	MBP Model
Recognition Rate	64.7%	81.7%	80.3%
Mean Score	0.461	0.474	0.470
Variance	0.488	0.428	0.430

Table 4. Recognition rate of same-session data under variations due to ambient temperature and metabolism

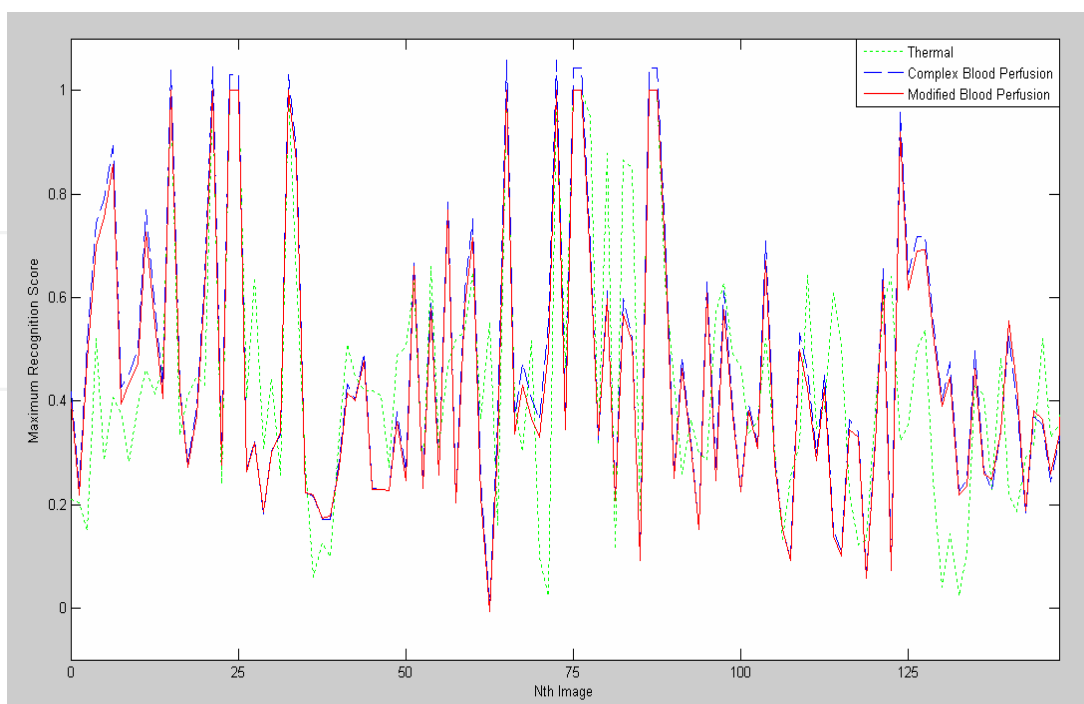


Fig. 13. Maximum recognition score for same-session data under variations due to ambient temperature and metabolism

variations due to ambient temperature and metabolism. In light of this, limitations are posed for recognition using thermal imaging. It is also observed that blood perfusion models try to alleviate these variations and yield reasonably performances. However, the recognition scores are relatively low and the variances are relatively high.

**C. Effect of breathing patterns**

In Sect 2.4, we analyzed the effects on thermal variation associated with breathing. Here, experiments are conducted to obtain the recognition results when the subject is inhaling, exhaling, followed by breathing normally. First, we performed the experiments when the subjects are inhaling. The number of probe images collected is 140. Table 5 illustrates the recognition rates obtained by the three different models and Fig. 14 shows the maximum recognition scores.

Ambient Condition	Data Type	Recognition Rate
24.3°C – 25.3 °C	Thermal	69.8%
	Complex Blood Perfusion	90.1%
	Modified Blood Perfusion	87.1%

Table 5. Recognition rate for same-session data when inhalation

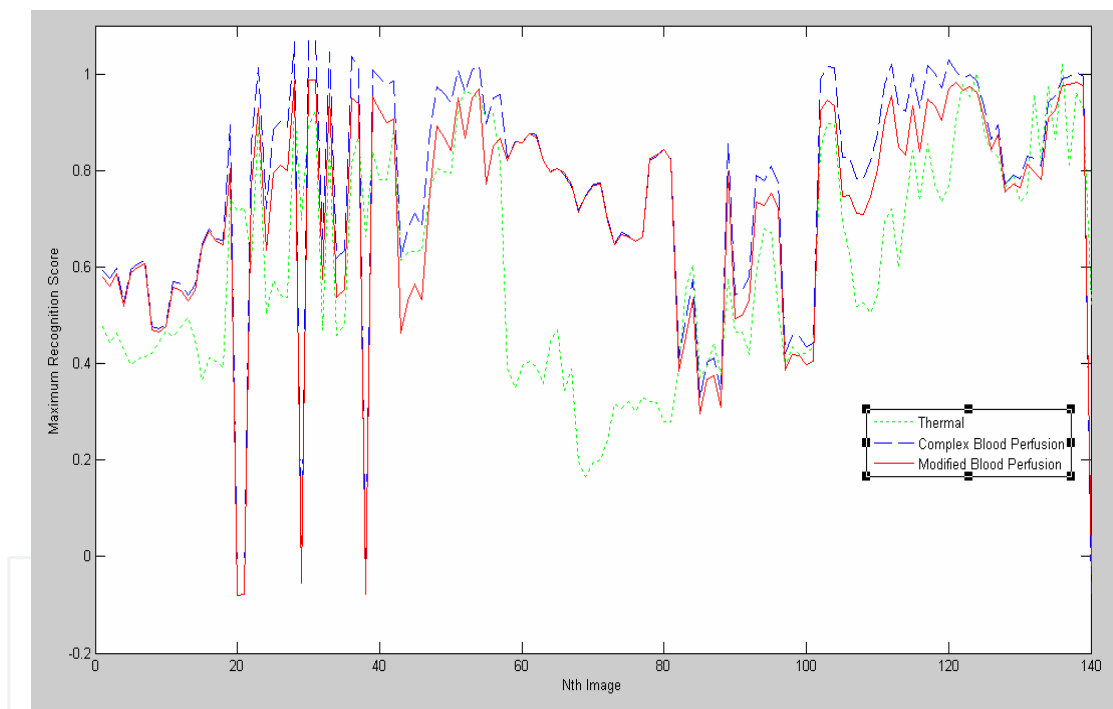


Fig. 14. Maximum recognition scores for same-session data when inhalation

In the next experiment, with the same group of people for test, they are instructed to only exhale during recognition. The total number of probe images in this case is 140. Table 6 shows the recognition rates and the recognition scores are depicted in Fig.15.

Ambient Condition	Data Type	Recognition Rate
24.3°C – 25.3 °C	Thermal	84.1%
	Complex Blood Perfusion	89.8%
	Modified Blood Perfusion	89.8%

Table 6. Recognition rate for same-session data when exhalation

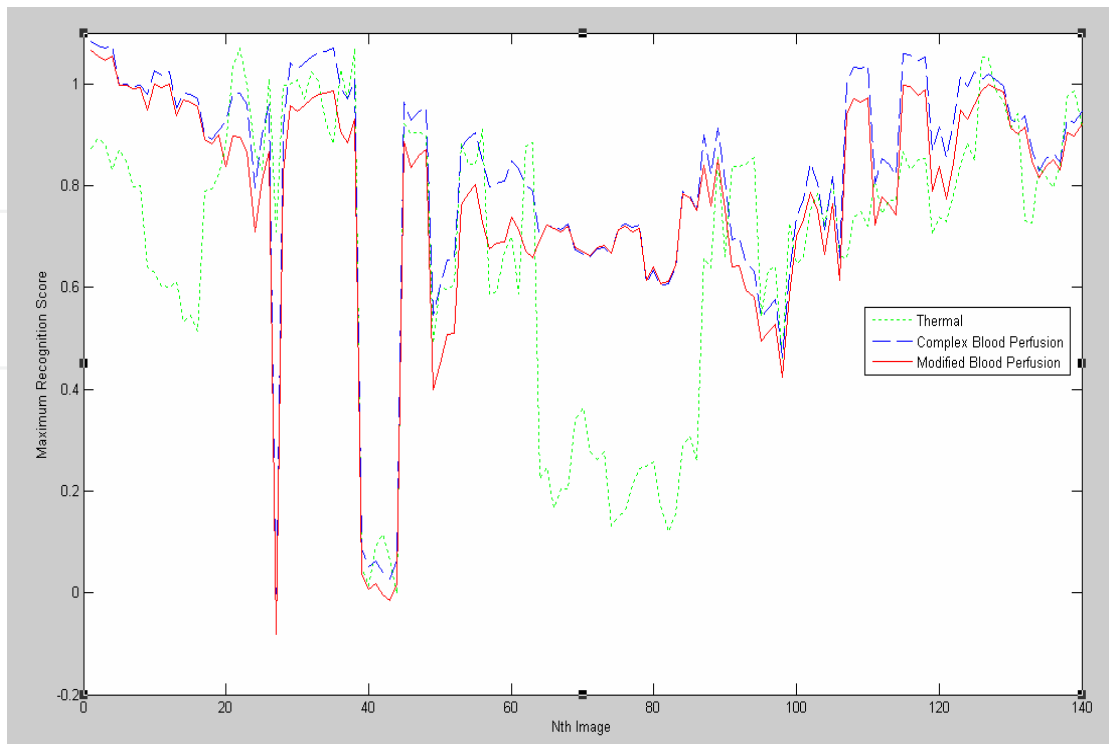


Fig. 15. Maximum recognition scores for same-session data when exhalation

The same group of people involved in the previous two breathing experiments is then instructed to breathe without any restraints in the next series of experiments. The number of probe images of subjects breathing normally is totally 135. The performances are shown in Table 7 and Fig. 16.

It is interesting to note how the recognition rates obtained from the thermal model vary under the three scenarios. It can be seen that the thermal model results in big change of performances (14.3%), and yields the best recognition rate result (84.1%) during the exhalation experiments. For both the blood perfusion models, the recognition rate results obtained from the three different scenarios are comparable, and yields the best recognition rate result (94.1%) during the normal breathing. This is further verified that the blood perfusion models are efficient.

#### D. Effect of hairstyle

It is also interesting to find the effect of hair on recognition performance as the hair/ hairstyle keeps change frequently. Table 8 and Fig. 17 illustrate the recognition results for a person with no hair, while Fig. 18 shows the recognition results for a female with long hair.

Ambient Condition	Data Type	Recognition Rate
24.3°C – 25.3 °C	Thermal	77.8%
	Complex Blood Perfusion	94.1%
	Modified Blood Perfusion	94.1%

Table 7. Recognition rate for same-session data when normal breathing

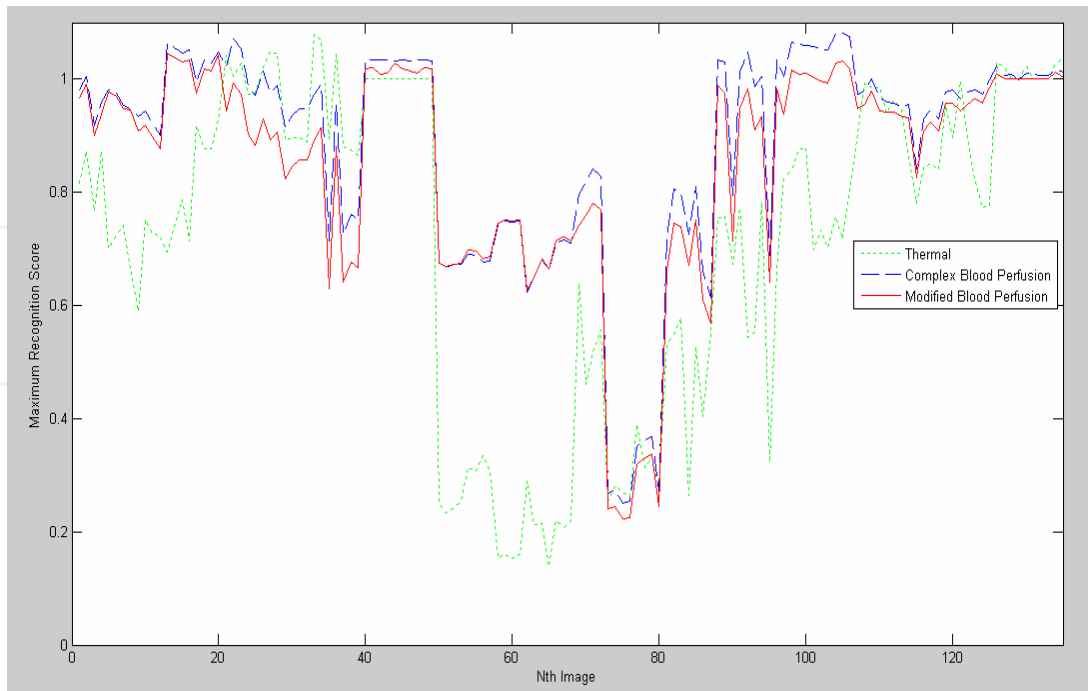


Fig. 16. Maximum recognition scores for same-session data when normal breathing

Ambient Condition	Thermal	OBP	MBP
24.3 °C – 25.3 °C	data	model	Model
Recognition Rate	80%	100%	100%
Mean Score	0.5132	0.6892	0.6632
Variance	0.3189	0.1853	0.1850

Table 8. Mean and variance of recognition scores for a bald subject

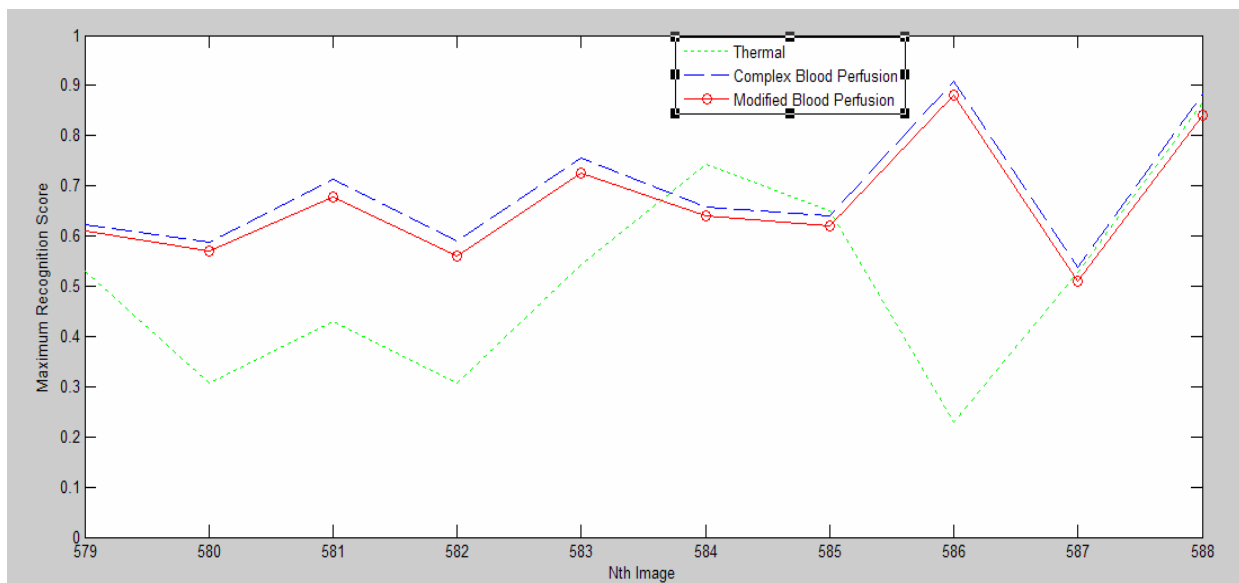


Fig. 17. Maximum recognition score for a bald subject

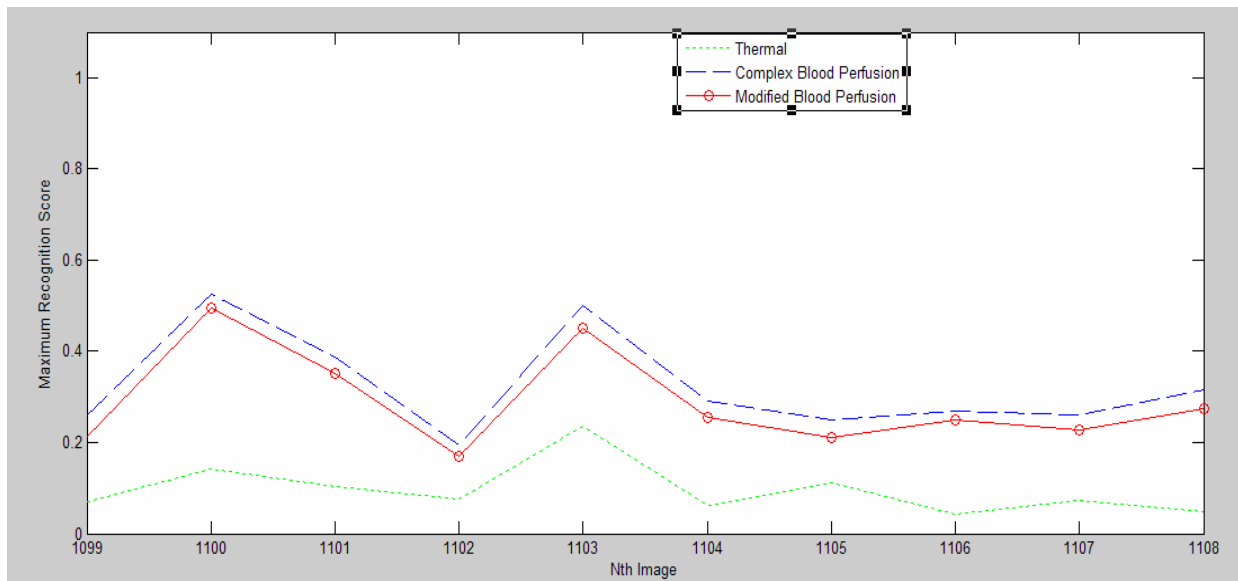
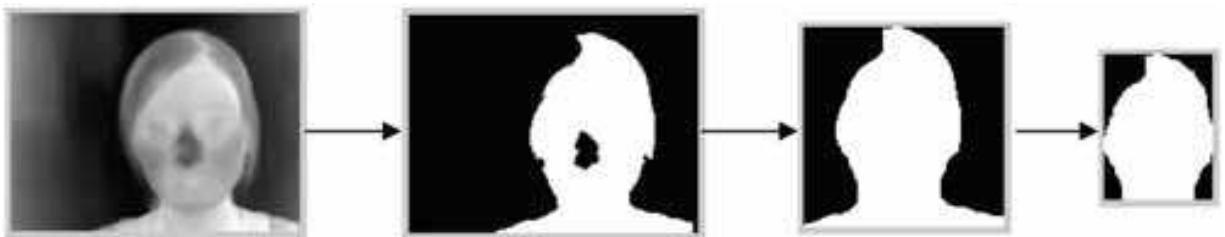


Fig. 18. Maximum recognition score for a female with long hair

Hair is an annoying factor for both segmentation and normalization of faces. As the thermal pattern of a face changes along with ambient temperature, psychological and physiological conditions, and the geometrical features of a face in an IR image is not clear, it is difficult to locate the facial features in IR images for face segmentation and normalization. In our recognition system (Wu et al., 2003), a face is segmented by temperature disparity between ambience and a face. Such method accordingly yields segmentation error by hair. Such situation is more serious for a female with long hair: for the same person, the segmentation results are significantly different caused by hair in different poses as shown in Figs. 19 and 20 respectively. On the other hand, hair is not a feature for recognition and accordingly affects performances. Therefore, the performance in terms of recognition rate and scores on subjects with bald head outperforms that on subjects with long hair.



Testing image acquired

Normalized image after face detection program

Fig. 19. Testing person with long hair: image 1 obtained after face detection program



Testing image acquired

Normalized image after face detection Program

Fig. 20. Testing person with hair: image 2 obtained after face detection program

It is interesting to find from Table 8 that 2 images are not recognized correctly for the bald subject when the thermal images are used, although the segmentation is excellent for such subjects as demonstrated in Fig.21. This is mainly caused by big pose variations. However, the 2 images can be recognized correctly by employing the proposed blood perfusion models.

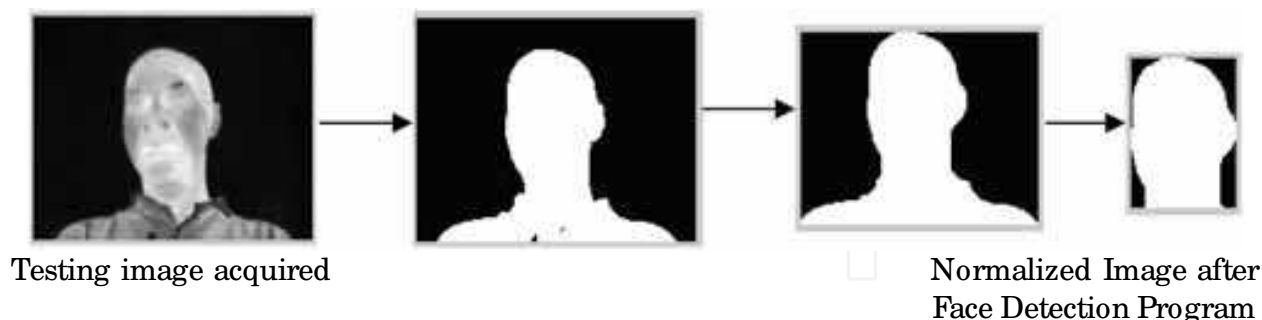


Fig. 21. Testing person with bald head: image obtained after face detection program

**E. Overall results for same-session data**

Considering all the aforementioned effects that can affect recognition performance, an overall recognition performance results based on same-session testing is generated. The number of subjects participating in this experiment is 85 and the number of probe images used here is 1780. Table 9 illustrates the overall results obtained.

These results illustrate that both the blood perfusion models are less sensitive to variations to the factors as aforementioned, than the thermal data. It can also be observed that the recognition rate obtained from the OBP model is only slightly better than that of the MBP model. This suggests that the MBP model not only aids in reducing complexity and the computational time, it can also perform as well as the OBP model for same-session data.

Ambient Condition	Model	Recognition Rate
24.3 °C – 25.3 °C	Thermal data	66.9%
	OBP model	86.6%
	MBP model	86.4%

Table 9. Recognition rate for same-session data

**4.4 Recognition results for time-lapse data**

Time-lapse recognition was conducted based on the data collected one month later. The testing situation and environmental condition are similar to that when collecting the training data, under the temperature ranging from 24.3 °C – 25.3 °C. The number of probe images is 180. The results obtained are indicated in Table 10 and Fig.22.

As the testing data were captured in air-conditioned room, it is considered that the testing individuals are in steady state without body temperature regulation. However, these time-lapse data comprise a variety of variations: ambient temperature (although it is small), face shape resulted from hair styles, and physiology etc. The effect of hair styles leads to inconsistency in face normalization, and accordingly results in decrease of recognition rate. However, we found that one crucial factor came from physiology, for example, relaxed in morning, and tired in afternoon and at night. It was shown that even the ambient temperature was almost the same, the face images collected when the person was overtired cannot be recognized at all, and the effect of physiology on recognition rate varies from person to person. It is the key reason to affect the performance identified on time-lapse data.

The experimental results shown in Table 10 and Fig.22 reveal that it is difficult to use the thermograms to identify the person accurately under time-lapse scenarios. The recognition rate, using temperature data, decreases significantly from 66.9% (for same-session data) to 23.8%. The performance using OBP model also yields big change ranged from 86.6% for same-session data to 76.6% for time-lapse data. However, it should be highlighted from Table 10 that the MBP model achieves better performance than the OBP model under time-lapse testing. The recognition rate (83.7%) on time-lapse data is comparable to that of same-session data. It is also observed from Fig. 22 that the scores performed on the MBP model is the highest amongst the three models at most times. Therefore, it is concluded that the MBP model is more suitable for real IR face recognition system.

Ambient Condition	Model	Recognition Rate
24.3 °C – 25.3 °C	Thermal data	23.8%
	OBP model	76.6%
	MBP model	83.7%

Table 10. Recognition rate for time-lapse data

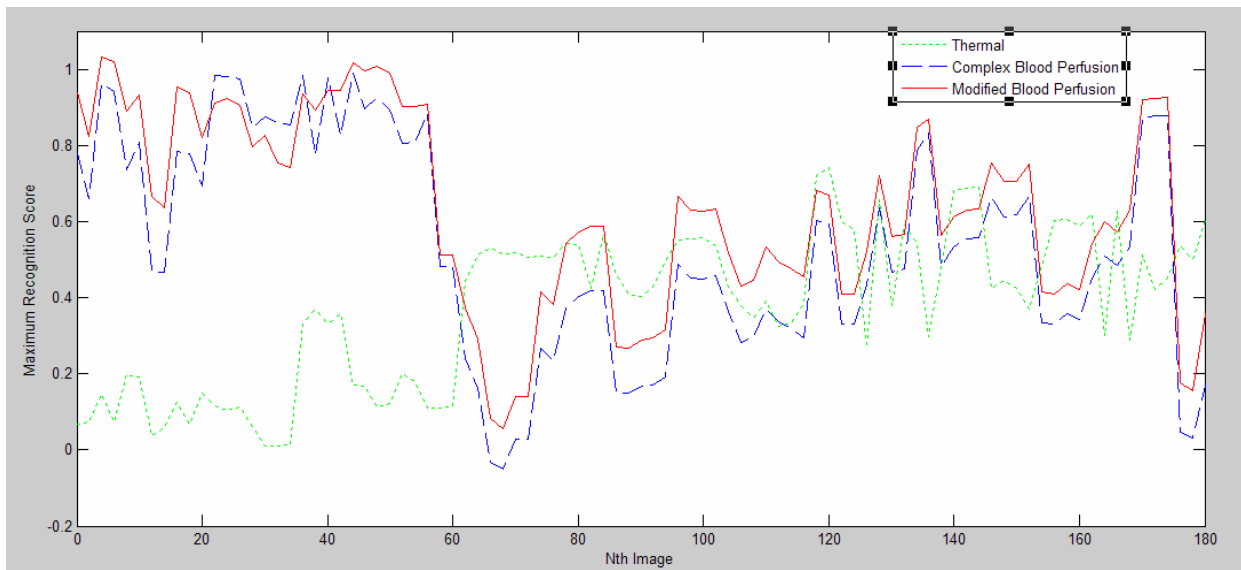


Fig. 22. Maximum recognition score for time-lapse data

## 5. Conclusion

Infrared imagery has been proposed for face recognition because it is independent on external illumination and shading problem. However, the thermal pattern of a face is also severely affected by a variety of factors ranging from eyeglasses, hairstyle, environmental temperature to changes in metabolism, breathing patterns and so on. To alleviate these variations, blood perfusion models are proposed to convert thermal information into physiological data. The transforms are nonlinearly monotonous, and are able to reduce the within-class scatter resulting from ambience, metabolism and so on, and more consistent features which represent the human faces are obtained. The extensive experiments demonstrated that the recognition performances with blood perfusion models are substantially better than that with thermal data in different situations, especially for time-lapse data.

It should be highlighted that physiological (e.g., fever) and psychological (e.g., happy, angry and sad etc) conditions also affect the thermal patterns of faces. Further analysis and experiments on these variations will be our future work.

## 6. References

- Blatteis, C. M. (1998). *Physiology and Pathophysiology of Temperature Regulation*, World Scientific Publishing Co
- Bone, M. & Blackburn, D. (2002). Face Recognition at a Chokepoint – Scenario Evaluation Results, [http://www.dodcounterdrug.com/facialrecognition/DLs/ChokePoint\\_Results.pdf](http://www.dodcounterdrug.com/facialrecognition/DLs/ChokePoint_Results.pdf), November 14, 2002
- Buddharaju, P.; Pavlidis I. & Kakadiaris I. A. (2004). Face recognition in the thermal infrared spectrum, *Proceedings of IEEE International Conference on Computer Vision and Pattern Recognition Workshop*, pp. 133-133, Washington DC, USA, 2004
- Buddharaju, P.; Pavlidis I. & Tsiamyrtzis, P. (2005). Physiology-based face recognition using the vascular network extracted from thermal facial images: a novel approach, *Proceedings of IEEE Advanced Video and Signal Based Surveillance*, pp. 354-359, Lake Como, Italy, 2005
- Chen, X.; Flynn, P. J & Bowyer, K. W. (2005). IR and visible light face recognition, *Computer Vision and Image Understanding*, Vol. 99, No. 3, pp. 332-358, 2005
- Ganong, W. F. (2001). *Review of Medical Physiology*, 20th ed., McGraw-Hill Medical Publishing Division
- Goodwin, D. W. (2000). *Alcoholism: the facts*, 3rd ed., Oxford University Press, USA
- Guyton, A. C. & Hall, J. E. (1996). *Textbook of Medical Physiology*, 9<sup>th</sup> ed., Philadelphia: W.B. Saunders Company, 1996
- Houdas, Y. & Ring, E. F. J. (1982). *Human Body Temperature: Its Measurement and Regulation*. New York: Plenum Press, 1982
- Jones, B. F. & Plassmann, P. (2002). Digital infrared thermal imaging of human skin, *IEEE Engineering in Medicine & Biology Magazine*, Vol. 21, No. 6, pp.41-48, 2002
- Kong, S. G.; Heo, J.; Abidi, B. R. Paik, J. & Abidi, M. A. (2005). Recent advances in visual and infrared race recognition - a review, *Computer Vision and Image Understanding*, Vol. 97, No. 1, pp. 103-135, 2005
- Prokoski, F. J.; Riedel, B. & Coffin, J. S. (1992). Identification of individuals by means of facial thermography, *Proceedings of IEEE Int. Conf. Security Technology, Crime Countermeasures*, pp. 120-125, Atlanta, USA, Oct. 1992
- Prokoski, F. J. (2000). History, current status, and future of infrared identification, *Proceedings of IEEE Workshop on Computer Vision beyond Visible Spectrum: Methods and Applications*, pp. 5-14, Hilton Head, SC, USA, 2000
- Prokoski, F. J. (2001). Method and apparatus for recognizing and classifying individuals based on minutiae, US Patent: 6173068B1, January 9, 2001.
- Socolinsky, D. A. & Selinger, A. (2002). A comparative analysis of face recognition performance with visible and thermal infrared imagery, *Proceedings of Int. Conf. Pattern Recognition*, pp. 217-222, Quebec, Canada, 2002
- Socolinsky, D. A. & Selinger, A. (2004A). Thermal face recognition in an operational scenario, *Proceedings of IEEE Conference on Computer Vision and Pattern Recognition*, pp. 1012-1019, Washington DC, USA, 2004

- Socolinsky, D. A. & Selinger, A. (2004B). Thermal face recognition over time, *Proceedings of Int. Conf. Pattern Recognition*, pp. 187-190, Cambridge, UK, 2004
- Srivastava, A. & Liu, X. (2003). Statistical hypothesis pruning for identifying faces from infrared images, *Image and Vision Computing*, Vol. 21, No. 7, pp. 651-661, 2003
- Wilder, J. Phillips, P. J.; Jang, C. & Wiener, S. (1996). Comparison of visible and infrared imagery for face recognition, *Proceedings of the 2<sup>nd</sup> Int. Conf. Automatic Face and Gesture Recognition*, pp. 182-187, Killington, Vermont, USA, 1996
- Wu, S. Q., Jang, L. J.; Cheng, L. et al. (2003). RIFARS: a real-time infrared face recognition system, *Proceedings of Asian Biometrics Workshop*, pp. 1-6, Singapore, 2003
- Wu, S. Q.; Song, W.; Jang, L. J et al. (2005A). Infrared face recognition by using blood perfusion data, *Proceedings of Audio- and Video-based Biometric Person Authentication*, pp. 320-328, Rye Brook, NY, USA, 2005
- Wu, S. Q.; Lin, W. S.; Jang, L. J et al. (2005B). An objective out-of-focus blur measurement, *Proceedings 5th Int. Conf. Inform., Comm. & Sign. Proc.*, pp. 334-338, Bangkok, Thailand, 2005
- Wu, S. Q.; Jang, L. J.; Xie, S. L. & Yeo, C. B. (2006) A robust method for detecting facial orientation in infrared images, *Patt. Recog.*, Vol. 39, No. 2, pp. 303-309, 2006
- Wu, S. Q.; Gu, Z. H.; Chia, K. A. & Ong, S. H. (2007). Infrared facial recognition using modified blood perfusion, *Proceedings 6th Int. Conf. Inform., Comm. & Sign. Proc.*, pp. 1-5, Singapore, Dec, 2007
- Yoshitomi, Y.; Miyaura, T.; Tomita, S. & Kimura, S. (1997). Face identification using thermal image processing, *Proceedings of IEEE Int. Workshop of Robot and Human Communication*, pp. 374-379, Sendai, Japan, 1997

IntechOpen



### **Recent Advances in Face Recognition**

Edited by Kresimir Delac, Mislav Grgic and Marian Stewart Bartlett

ISBN 978-953-7619-34-3

Hard cover, 236 pages

**Publisher** InTech

**Published online** 01, June, 2008

**Published in print edition** June, 2008

The main idea and the driver of further research in the area of face recognition are security applications and human-computer interaction. Face recognition represents an intuitive and non-intrusive method of recognizing people and this is why it became one of three identification methods used in e-passports and a biometric of choice for many other security applications. This goal of this book is to provide the reader with the most up to date research performed in automatic face recognition. The chapters presented use innovative approaches to deal with a wide variety of unsolved issues.

#### **How to reference**

In order to correctly reference this scholarly work, feel free to copy and paste the following:

Shiqian Wu, Zhi-Jun Fang, Zhi-Hua Xie and Wei Liang (2008). Blood Perfusion Models for Infrared Face Recognition, *Recent Advances in Face Recognition*, Kresimir Delac, Mislav Grgic and Marian Stewart Bartlett (Ed.), ISBN: 978-953-7619-34-3, InTech, Available from:

[http://www.intechopen.com/books/recent\\_advances\\_in\\_face\\_recognition/blood\\_perfusion\\_models\\_for\\_infrared\\_face\\_recognition](http://www.intechopen.com/books/recent_advances_in_face_recognition/blood_perfusion_models_for_infrared_face_recognition)

# **INTECH**

open science | open minds

#### **InTech Europe**

University Campus STeP Ri  
Slavka Krautzeka 83/A  
51000 Rijeka, Croatia  
Phone: +385 (51) 770 447  
Fax: +385 (51) 686 166  
[www.intechopen.com](http://www.intechopen.com)

#### **InTech China**

Unit 405, Office Block, Hotel Equatorial Shanghai  
No.65, Yan An Road (West), Shanghai, 200040, China  
中国上海市延安西路65号上海国际贵都大饭店办公楼405单元  
Phone: +86-21-62489820  
Fax: +86-21-62489821

© 2008 The Author(s). Licensee IntechOpen. This chapter is distributed under the terms of the [Creative Commons Attribution-NonCommercial-ShareAlike-3.0 License](#), which permits use, distribution and reproduction for non-commercial purposes, provided the original is properly cited and derivative works building on this content are distributed under the same license.

IntechOpen

IntechOpen